

## Nano-scale grain growth kinetics

Feng Liu\*, Gencang Yang, Haifeng Wang, Zheng Chen, Yaohe Zhou

State Key Laboratory of Solidification Processing, Northwestern Polytechnical University, Xi'an, Shaanxi 710072, PR China

Received 7 December 2005; received in revised form 13 January 2006; accepted 24 January 2006

Available online 28 February 2006

### Abstract

An empirical relation among three important properties of grain boundary (GB), i.e. GB free energy, energy change of GB segregation, and GB excess, was shown. Accordingly, GB energy reduces with grain growth. Once GB energy is equal to zero, GBs will be in thermodynamic equilibrium in the presence of solute atoms and, therefore, grain growth stops with saturated GBs. Applying a kinetic model for nano-scale grain growth, some published experimental data were successfully reinterpreted. With progressing grain growth, the activation energy of grain growth increases, in contrast with the reduction of GB energy. In connection with a semi-empirical relation according to the conjecture that GB energy is the difference between those responsible for diffusion in the lattice and the GB itself, proposed by Borisov, a conclusion can be drawn that, for alloy with strong segregation tendency, grain growth is inhibited due to the reduction of GB energy, even to zero.

© 2006 Elsevier B.V. All rights reserved.

**Keywords:** Nano-scale; Grain growth; Grain boundary; Diffusion

### 1. Introduction and theory background

Generally, grain growth occurs in polycrystalline materials to decrease the system free energy by decreasing the total grain boundary (GB) energy. Analogous to the growth of cells in soap froth, GB moves toward its centre of curvature and the rate of movement varies with the amount of curvature. The earliest theoretical consideration of the kinetics of normal grain growth assumes a linear relationship between the growth rate and the inverse grain size, which is proportional to the radius of the grain [1,2].

$$\frac{dD}{dt} = \frac{k}{D} \quad (1)$$

where  $D$  is the mean grain diameter after an annealing time  $t$ , and  $k$  a temperature-dependent rate constant. The integration of Eq. (1) and the determination of the integration constant as the grain size  $D_0$  (the initial grain size) yields, under ideal conditions.

$$D^2 - D_0^2 = kt \quad (2)$$

A number of recent theoretical treatments came to the same conclusion that the normal grain growth should ideally occur in a

parabolic manner. However, this is rarely observed except for high purity metals at high homologous temperatures. For practical purpose, the most widely used relationship incorporates the empirical time constant,  $n < 0.5$ , which allows the description of isothermal grain growth that often does not fit Eq. (2) [1]:

$$D_t^{1/n} - D_0^{1/n} = k't \quad \text{or} \quad D_t = (k't + D_0^{1/n})^n \quad (3)$$

In the case of materials with lower purity and/or alloying with certain solutes, the long-time grain growth shows a stagnation which is supposed to be associated with the pinning effect of GB by the second-phase particles, impurities, pores and surfaces [1,2]. Burke introduced a maximal grain size,  $D_{\max}$ , to account for the above pinning effect on GB mobility, and by assuming a constant pinning force, an equation for isothermal grain growth is obtained as [1]:

$$\frac{D_0 - D_t}{D_{\max}} + \ln \left[ \frac{D_{\max} - D_0}{D_{\max} - D_t} \right] = \frac{k}{D_{\max}^2} t \quad (4)$$

For nano-crystalline alloys, the large change of the total GB area accompanying grain growth would greatly affect the grain growth kinetics. As GB area diminishes, the concentration of solute or impurity atoms segregated to the GBs is expected to increase, and introduces a grain-size dependent retarding force on GB migration. On this basis, Michels et al. obtained the fol-

\* Corresponding author.

E-mail address: [liufeng@nwpu.edu.cn](mailto:liufeng@nwpu.edu.cn) (F. Liu).

lowing grain growth equation [3]:

$$D_t = \left\{ D_{\max}^2 - (D_{\max}^2 - D_0) \exp\left(-\frac{2kt}{D_{\max}^2}\right) \right\}^{1/2} \quad (5)$$

From Eqs. (1)–(5), it can be inferred that the GB energy hold constant throughout the grain growth.

The stability of nano-crystalline alloys with respect to grain growth is thoroughly discussed. Some authors [3–5] claimed that solute drag by the alloying or impurity atoms reduces the GB mobility, whereas others attributed it to a vanishing driving force [6–8], i.e. the GB energy. According to the Gibbs adsorption equation [9,10] and the thermodynamic treatment by Weissmuller et al. [6] and Kirchheim and co-workers [8,11], the GB energy,  $\sigma_b$ , reduces with solute segregation. If it is possible to reduce  $\sigma_b$  to zero or negligible values, then there would be no driving force for grain growth or coarsening in such a solid.

$$\sigma_b = \sigma_0 - \Gamma_{b0} RT \ln X_0 + \Delta H_{\text{seg}} \quad (6)$$

where  $\sigma_0$  is the GB energy for pure solvent,  $X_0$  the bulk content,  $\Gamma_{b0}$  ( $=X_b d \rho$  with  $X_b$ ,  $d$  and  $\rho$  as the concentration, the width and the density of GB [11] at saturation) the solute excess of GB monolayer available for segregation at saturation, and  $\Delta H_{\text{seg}}$  the energy change of segregation per mole of solute. Whenever  $\sigma_b$  is positive, grain growth will decrease the free energy of the system. Since systems with  $\sigma_b < 0$  are not thermodynamically stable, the only case where grain growth can be suppressed is where  $\sigma_b = 0$ .

For nano-scale materials, grain growth is accompanied by a reduction in diffusion, i.e. an increase of activation energy ( $Q$ ) of diffusion [12]. Upon grain growth,  $Q$  should be increased, in contrast with a reduction of  $\sigma_b$ . Only if grain growth stops with saturated GBs,  $\sigma_b$  could be zero [8,11]. Approximately, a single grain growth process can be separated as several domains, where  $Q$  and  $\sigma_b$  hold constant within each domain [13].

$$\begin{aligned} \int_{D_0}^{D_n} D \, dD &= \int_{D_0}^{D_1} D \, dD + \dots + \int_{D_{n-1}}^{D_n} D \, dD \\ &= \int_0^{t_1} [A_1 \sigma_{b1}] \exp\left(-\frac{Q_{b1}}{RT}\right) dt + \dots \\ &\quad + \int_{t_{n-1}}^{t_n} \left[ A_n \sigma_{bn} \exp\left(-\frac{Q_{bn}}{RT}\right) \right] \end{aligned} \quad (7)$$

where  $A_1 \dots A_n$  is constant, and  $\sigma_{b1} > \sigma_{b2} \dots > \sigma_{bn}$  and  $Q_{b1} < Q_{b2} \dots < Q_{bn}$  with  $n$  as the number of domains. Integration of Eq. (7) gives

$$D_n^2 - D_0^2 = k_1 t_1 + k_2 (t_2 - t_1) + \dots + k_n (t_n - t_{n-1}) \quad (8)$$

with  $k_1 > k_2 \dots > k_n$ . For practical usage, Eq. (8) can be rewritten as [13]:

$$D_t^2 - D_0^2 \left\{ \begin{array}{l} k_1 t \quad t \leq t_1 \\ k_1 t_1 + k_2 (t - t_1) \quad t_2 > t > t_1 \\ \dots \\ \dots \\ k_1 t_1 + k_2 (t_2 - t_1) + \dots + k_n (t - t_{n-1}) \quad t_n > t > t_{n-1} \end{array} \right\} \quad (9)$$

Apparently, higher value of  $n$  gives better fits to the experimental data. Generally,  $n$  can be chosen as 2 or 3.

The phenomenon that can be described using Eqs. (6)–(9) is especially interesting in nano-materials because the total GB area is very large and a large driving force for grain growth is expected. In this article, we aim to prove nano-scale grain growth is inhibited by reducing GB energy through solute segregation, and, for alloy with strong segregation tendency, grain growth stops with saturated GBs with zero GB energy.

## 2. Experimental interpretations

### 2.1. Nano-scale grain growth in Pd<sub>81</sub>Zr<sub>19</sub> alloy

In order to verify that the activation energy increases with grain growth, the experimental data of grain growth in the nano-crystalline Pd<sub>81</sub>Zr<sub>19</sub> alloy produced by mechanical alloying [4] was adopted. Fig. 1a and b show fits of Eq. (9) ( $n=2$  and 3) and Eq. (5) to the measured data points. Accordingly, fits of Eq. (5) gives one average activation energy,  $Q$  ( $k=0.0067 \text{ nm}^2/\text{s}$ , the relative errors of fit is equal to 3.1%), whereas fits of Eq. (9) results in two activation energies,  $Q_1$  and  $Q_2$  ( $k_1^2 = 0.0094 \text{ nm}^2/\text{s}$  and  $k_2^2 = 0.00087 \text{ nm}^2/\text{s}$ , the relative errors of fit is equal to 2.5%), and three activation energies,  $Q_1$ ,  $Q_2$  and  $Q_3$  ( $k_1^3 = 0.0080 \text{ nm}^2/\text{s}$ ,  $k_2^3 = 0.0019 \text{ nm}^2/\text{s}$  and  $k_3^3 = 0.00015 \text{ nm}^2/\text{s}$ , the relative errors of fit is equal to 1.5%), for  $n=2$  and 3, respectively. From the relative errors, Eq. (9) describes grain growth in the nano-crystalline Pd<sub>81</sub>Zr<sub>19</sub> alloy better.

As is shown,  $k \cong k_1^2 \cong k_1^3 > k_2^2 \cong k_2^3 > k_3^3$  (cf. Eq. (9)). This implies that, the activation energy of the second or the third growth domain,  $Q_2$  or  $Q_3$ , is higher than the activation energy of the first growth domain,  $Q_1$ . From [4], the Zr concentration segregated to the Pd GBs,  $C_{\text{Zr}}^{\text{gb}}$ , was found to increase with progressing grain growth; once grain size reaches 15–16 nm, grain growth stops with the maximal  $C_{\text{Zr}}^{\text{gb}}$  as 26 at.%. Suppose the GB width to be 0.8 nm [5,14], the GB excess (see below Eq. (6)) was calculated to be  $2.7\text{--}2.8 \times 10^{-5} \text{ mol/m}^2$ , which corresponds to the saturated monolayer-segregation [6,10,11,13,15] and the maximal activation energy of grain growth [12].

It should be noted that the Pd<sub>81</sub>Zr<sub>19</sub> alloy considered here is different from that considered in [11]. Here, we focused on the isothermal grain growth, whereas the evolution of grain size with the annealing temperatures and alloy contents was considered in [11].

### 2.2. Grain growth in nano-crystalline RuAl

Subjected to annealings at different temperatures (873–1273 K), the grain size,  $D$ , of nano-crystalline RuAl

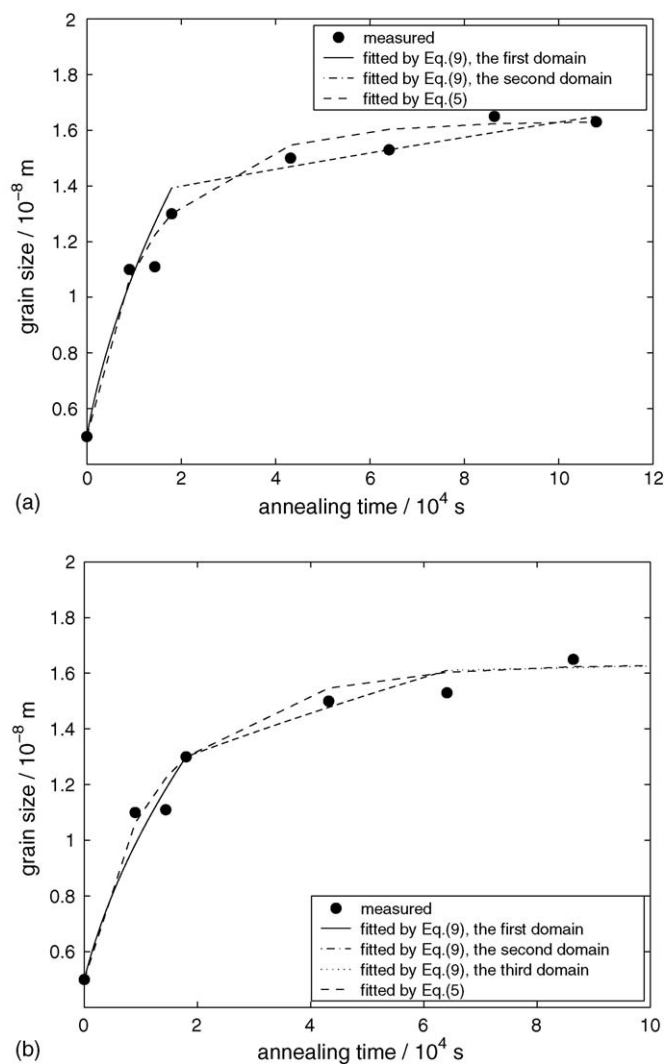


Fig. 1. Comparison of fits using Eq. (5) and using Eq. (9) ((a)  $n=2$  and (b)  $n=3$ ) to the grain sizes measured in nano-crystalline Pd<sub>81</sub>Zr<sub>19</sub> alloy prepared by mechanical alloying, at an annealing temperature of 873 K [4].

produced by mechanical alloying [5], was evaluated as a function of annealing time,  $t$  (see Fig. 2). After certain annealing time, grain growth stagnates and  $D$  reaches the maximal value. As shown in Fig. 2, both Eq. (5) and Eq. (9) ( $n=2$  and 3) give good fits to the experimental data points. The fitting results were given in Table 1. Since the values of  $k_2$  and  $k_3$  are much larger than that of  $k_1$ , a detail investigation of the rate constants is needed. Assume that the rate constant  $k$  has an Arrhenius

Table 1  
Values of the rate constant obtained from fits of Eqs. (5) and (9) ( $n=2$  and 3) to the measured data points of Fig. 2

$T$ (K)	Eq. (5)		Eq. (9)			Michels' model		Error	
	$k_1$ (nm <sup>2</sup> /s)	$k_2$ (nm <sup>2</sup> /s)	$k_1$ (nm <sup>2</sup> /s)	$k_2$ (nm <sup>2</sup> /s)	$k_3$ (nm <sup>2</sup> /s)	$D_{\max}$ (nm) [5]	$k$ (nm <sup>2</sup> /s) [5]	$n=2$	$n=3$
873	0.021	0.00002				10.3	0.029	1.7	
973	0.032	0.00038				13.1	0.048	2.3	
1073	0.072	0.0035	0.068	0.011	0.00098	18.7	0.076	2.6	1.3
1173	0.28	0.023	0.33	0.035	0.0025	39.0	0.16	2.4	0.9
1273	1.47	0.11	1.26	0.33	0.067	83.1	0.93	2.7	1.4

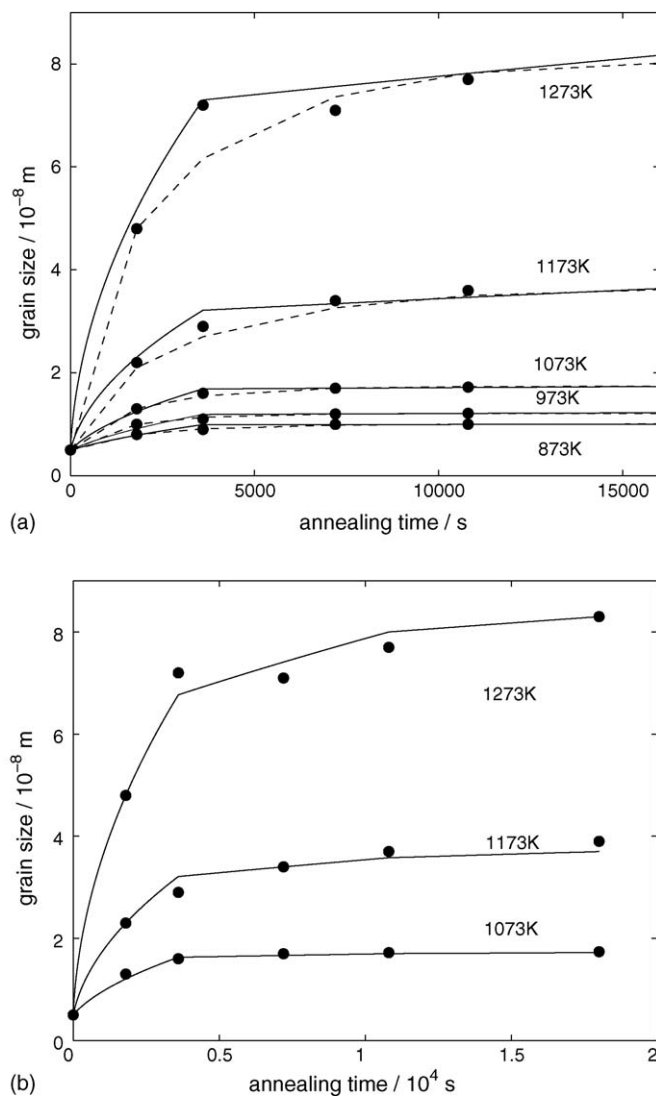


Fig. 2. Fits using Eqs. (5) (dashed line) and (9) (solid line) ((a)  $n=2$  and (b)  $n=3$ ) to the grain sizes measured in nano-crystalline RuAl alloy [5] produced by mechanical alloying, at different annealing temperatures.

relation with temperature.

$$k = k_0 \exp \left[ -\frac{Q}{RT} \right] \quad (10)$$

where  $R$  is the gas constant,  $T$  the absolute temperature, and  $k_0$  a constant. The activation energy can be deduced from the slope of a plot of  $\ln k$  against  $1/T$ . The results are shown in Fig. 3.

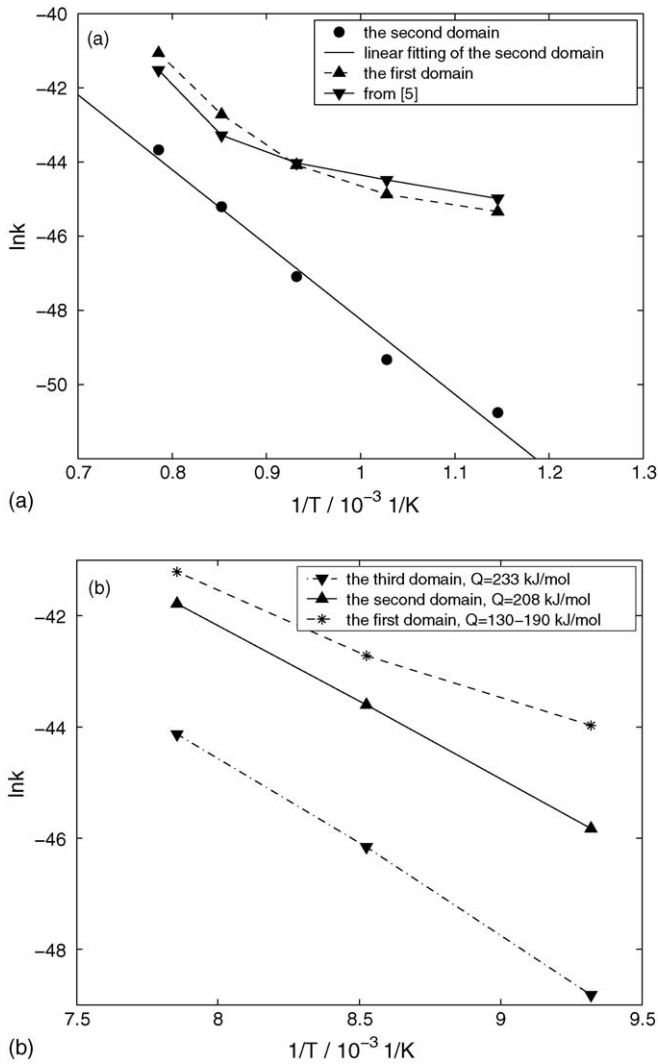


Fig. 3. Arrhenius plot of logarithm of the rate constants:(a)  $k$  (by Eq. (5)) and  $k_1$  and  $k_2$  (by Eq. (9),  $n=2$ ) and (b)  $k_1$ ,  $k_2$  and  $k_3$  (by Eq. (9),  $n=3$ ), against the reciprocal annealing temperature.

Obviously, it is impossible to fit the data points derived from  $k$  (by Eq. (5)) and  $k_1$  (by Eq. (9)) with a straight line. The only possible way is to obtain the slope of neighbouring points for each temperature range. So the deduced activation energy of grain growth,  $Q$  (by Eq. (5)) or  $Q_1$  (by Eq. (9)) dramatically increases upon increasing annealing temperature (Table 2). As for the second and the third domains, nearly straight lines result,

according to the relations of  $\ln k_2$  against  $1/T$  and  $\ln k_3$  against  $1/T$ .

Unfortunately, the grain growth at lower temperatures (973 and 873 K) stagnates so early that we cannot obtain the reliable, regular, values for the rate constant,  $k_3$ , as has been obtained for the three higher temperatures.

### 3. Discussion

In the pure-metal nano-crystalline samples of Cu and Ag, it has been observed that the activation energy for grain growth corresponds to the typical value for GB diffusion. However, if the samples contain some gaseous impurities such as oxygen, the activation energy for grain growth will be enhanced. It was found that the value of the activation energy of grain growth in an Ag–7 at.% O nano-crystalline sample is about 210 kJ/mol [16], which is even a little bit higher than the activation energy of volume self-diffusion in pure Ag (i.e. about 197 kJ/mol). The investigation in GB self-diffusion in Cu polycrystal of different purity showed that increasing the GB impurity concentration leads to a decrease in GB energy, while enhancing the activation energy for GB self-diffusion [17]. This is compatible with the theoretical interpretation shown in Section 2, i.e. increasing the annealing temperature strengthens solute segregation, and thus increases the activation energy of grain growth (see Table 2). From the relation of  $\ln k_1$  against  $1/T$ , one can expect a continuous increase of  $Q_1$  from 32.3 to 190 kJ/mol, which indicates a strengthened solute segregation with increasing  $T$ . From the relations of  $\ln k_2$  against  $1/T$  and  $\ln k_3$  against  $1/T$ , the activation energies for grain growth in the second and third domains,  $Q_2$  and  $Q_3$ , were deduced to be 216 or 208 and 233 kJ/mol (Fig. 3b and Table 2), respectively.

With reference to Eq. (9), GB energy reduces with grain growth, and thus high stability results from the reduced GB energy (see Fig. 2). This could be ascribed to the increased activation energy of GB diffusion due to the strengthened solute segregation with grain growth.

Borisov et al. had related the increased atomic mobility in GB self-diffusion to the interfacial energy associated with the GBs in a semi-empirical manner from which one can be determined if the other is known [18]. The basic postulate in their approach is that the Gibbs free energy of an atom-vacancy jump in the GBs,  $\Delta G_b$ , to the first approximation, is reduced by the absolute GB energy,  $\sigma_b$ , from its level in the lattice,  $\Delta G_l$ . Accordingly, the GB energy is equal to the difference between

Table 2  
Grain growth activation energies for different temperature ranges deduced from the slope of a plot of  $\ln k$  against  $1/T$  (see Fig. 3)

Temperature range (K)	Eq. (5) [5]	Eq. (9), $n=2$		Eq. (9), $n=3$		
	$Q$ (kJ/mol)	$Q_1$ (kJ/mol)	$Q_2$ (kJ/mol)	$Q_1$ (kJ/mol)	$Q_2$ (kJ/mol)	$Q_3$ (kJ/mol)
873–973	39.2	32.3				
973–1073	40.3	69.5				
1073–1173	73.1	122.1	216	130	208	233
1173–1273	213.5	189		190		

the free energy of activation for diffusion in the lattice and in the GB [19].

$$\sigma_b = \left( \frac{RT}{2a_0^2 N_A} \right) \left[ \ln \left( \frac{D_b}{D_1} \right) \right] = \Delta G_1 - \Delta G_b \quad (11)$$

where  $a_0$  is the inter-atomic distance,  $N_A$  Avogadro's number,  $D_1$  the volume self-diffusion coefficient, and  $D_b$  the GB self-diffusion coefficient. To stop grain growth with saturated GBs with  $\sigma_b = 0$  requires the difference between  $D_b$  and  $D_1$  or between  $\Delta G_b$  and  $\Delta G_1$  be negligible as a result of solute segregation and grain growth.

Unfortunately, we can only obtain the values of the activation energy of Al volume self-diffusion, 144 kJ/mol, and the activation energy of Ru tracer-diffusion in Fe, 244 kJ/mol [20]. In connection with Fig. 2 and Table 2, approximately, the activation energy of GB self-diffusion when grain growth stagnates can be assumed to be close to the activation energy of volume self-diffusion in nano-RuAl.

For alloy system with strong segregation tendency, the grain growth is inhibited by reducing the GB energy. If the combined effects of solute segregation and grain growth realize a possible equivalence between the activation energy for grain growth and the activation energy for volume self-diffusion, grain growth is suppressed with zero GB energy corresponding to saturated GBs (cf. Eq. (9)).

#### 4. Conclusion

With reference to an empirical relation derived from Gibbs adsorption equation and Mclean's grain boundary segregation model, the grain boundary energy and the activation energy for grain growth change with grain growth. On this basis, a kinetic model for nano-scale grain growth is adopted to fit to some published experimental data. According to the fitting results, it was found that the thermodynamic description using Eq. (9) provides a better description for nano-scale grain growth than the kinetic one by Eq. (5). In connection with the empirical relation between grain boundary energy and activation energy for grain boundary self-diffusion, proposed by Borisov, it can be proved that for some alloy systems with strong segregated tendency, grain boundary energy can

reduce to zero, while grain growth stops with saturated grain boundaries.

#### Acknowledgements

This research is supported by the Alexander von Humboldt Foundation. The authors are grateful to the National Natural Science Foundation of China for the financial support under grant No.50501020 and 50395103, and the Science and Technology Creative Fund of Youth in Northwestern Polytechnical University.

#### References

- [1] J.E. Burke, *Trans. AIME* 73 (1949) 180.
- [2] H.V. Atkinson, *Acta Mater.* 36 (1988) 469.
- [3] C.H. Moelle, H.J. Fecht, *Nanostruct. Mater.* 6 (1995) 421.
- [4] A. Michels, C.E. Krill, H. Ehrhardt, R. Birringer, D.T. Wu, *Acta Mater.* 47 (1999) 2143.
- [5] K.W. Liu, F. Mücklich, *Acta Mater.* 49 (2001) 395.
- [6] J. Weissmüller, W. Krauss, T. Haubold, R. Birringer, H. Gleiter, *Nanostruct. Mater.* 1 (1992) 439.
- [7] J. Weissmüller, *Nanostruct. Mater.* 3 (1993) p.261.
- [8] R. Kirchheim, *Acta Mater.* 50 (2002) 413.
- [9] (a) J.W. Gibbs, *Trans. Conn. Acad.* III (1876) 108–248;  
(b) J.W. Gibbs, *Trans. Conn. Acad.* III (1878) 343–524;  
(c) J.W. Gibbs (Ed.), *The Collected Works*, vol. 1, Longmans, Green and Co., New York, 1928, pp. 55–354.
- [10] J.W. Cahn, in: W.C. Johnson, J.M. Blakely (Eds.), *Surface Segregation in Metals and Alloys*, ASM, Metals Park, 1979.
- [11] F. Liu, R. Kirchheim, *J. Cryst. Growth* 264 (2004) 385.
- [12] H.J. Höfler, R. Tao, L. Kim, R.S. Averbach, C.J. Altstetter, *Nanostruct. Mater.* 6 (1995) 901.
- [13] F. Liu, R. Kirchheim, *Thin Solid Films* 464 (2004) 108.
- [14] B. Färber, E. Cadel, A. Menand, G. Schmitz, R. Kirchheim, *Acta Mater.* 48 (2000) 789.
- [15] F. Liu, R. Kirchheim, *Scripta Mater.* 51 (2004) 521.
- [16] A. Kumpmann, B. Günther, H.D. Kunze, *Mater. Sci. Eng. A168* (1993) 165.
- [17] T. Surholt, C.H.R. Herzig, *Acta Mater.* 45 (9) (1997) 3817.
- [18] V.T. Borisov, V.M. Golikov, G.V. Scherbedinskiy, *Fiz. Met. Metall.* 17 (1964) 80.
- [19] D. Gupta, J. Oberschmidt, in: M.A. Dayananda, G.E. Murch (Eds.), *Diffusion in Solids: Recent Developments*, The Met. Soc. of AIME, New York, 1985.
- [20] C.J. Smithells, *Metal Reference Handbook*, sixth ed., Butterworths, London, 1986.